Development 127, 4645-4654 (2000)
Printed in Great Britain © The Company of Biologists Limited 2000
DEV3239

FIGα, a germ cell-specific transcription factor required for ovarian follicle formation

Selma M. Soyal*, Asma Amleh and Jurrien Dean

Laboratory of Cellular and Developmental Biology, NIDDK, National Institutes of Health, Bethesda, MD 20892, USA
*Author for correspondence: (e-mail: ss278v@nih.gov)

Accepted 11 August; published on WWW 9 October 2000

SUMMARY

Primordial follicles are formed perinatally in mammalian ovaries and at birth represent the lifetime complement of germ cells. With cyclic periodicity, cohorts enter into a growth phase that culminates in ovulation of mature eggs, but little is known about the regulatory cascades that govern these events. FIGα, a transcription factor implicated in postnatal oocyte-specific gene expression, is detected as early as embryonic day 13. Mouse lines lacking FIGα were established by targeted mutagenesis in embryonic stem cells. Although embryonic gonadogenesis appeared normal, primordial follicles were not formed at birth, and massive depletion of oocytes resulted in shrunken ovaries and female sterility. *Figα* (the gene for FIGα) null males have normal fertility. The additional observation that null females do not express *Zp1, Zp2* or *Zp3* indicates that FIGα plays a key regulatory role in the expression of multiple oocyte-specific genes, including those that initiate folliculogenesis and those that encode the zona pellucida required for fertilization and early embryonic survival. The persistence of FIGα in adult females suggests that it may regulate additional pathways that are essential for normal ovarian development.

Key words: Primordial follicles, Germ-line transcription factor, Factor in the germline, alpha (FIGα)

INTRODUCTION

Ovarian gonadogenesis in mammals is dependent on complex interactions between cells of at least four lineages: germ cells required for propagation of the species; supporting granulosa cells; theca cells for steroid production; and connective tissue (Capel, 1998). Postnatally, the ovary plays crucial roles in defining the female phenotype and in maturing oocytes into eggs during folliculogenesis in preparation for fertilization. Folliculogenesis requires careful orchestration of developmental programs in germ and somatic cells, as well as interactions between them. Perinatally, oocytes (approx. 12 μm) arrest in the prophase of the first meiotic division and become surrounded by single layers of flattened granulosa cells to form primordial follicles (Brambell, 1928). At birth, the mouse ovary contains 10,000-15,000 of these follicles, cohorts of which are induced to enter into a growth phase culminating in ovulation of eggs into the oviduct (Brambell, 1928; Peters, 1969). Little is known about the molecular mechanisms that lead to the initial formation of follicles, or the signals that stimulate growth of some follicles while others remain quiescent in the ovary for up to two years.

In the initial stages of folliculogenesis paracrine factors promote growth of the oocyte and adjacent somatic cells (Kol and Adashi, 1995). The granulosa cells become cuboidal in primary follicles and proliferate to form multilayers of somatic cells that surround oocytes in secondary follicles. In the absence of gonadotrophins (Halpin et al., 1986), these follicles become atretic and disappear from the ovary. After puberty, gonadotrophins stimulate further follicular growth and a fluid-filled cavity forms in the early antral follicle. This antrum enlarges dramatically and preovulatory follicles reach diameters of 400-600 μm. Although meiotically competent at this stage, oocytes are held in arrest by their interactions with granulosa cells (Pincus and Enzmann, 1935) until the preovulatory follicle stage, at which time they progress to metaphase II in anticipation of ovulation and subsequent fertilization.

The observation that rodents deficient in oocytes, owing to genetic mutations or chemical ablation, are also deficient in follicles (Columbre and Russell, 1954; Hirshfield, 1994) suggests that oocytes play crucial roles in the growth and development of the follicle. Factors that direct the initial formation of follicles remain unknown, but are thought to involve complex interactions between oocytes and the surrounding somatic cells (Eppig, 1991). FIGα (factor in the germline, alpha), a germ cell-specific, basic helix-loop-helix (bHLH) factor, has been implicated in the coordinate expression of the three zona genes (*Zp1*, *Zp2* and *Zp3*) that encode the mouse egg coat (Liang et al., 1997). Due to the economy of developmental systems, transcription factors are often used for more than one function. By establishing mouse lines lacking FIGα, we now confirm a requirement for this bHLH transcription factor in zona gene expression and, in addition, report its crucial requirement in the initial formation of primordial follicles, without which female mice are sterile.

MATERIALS AND METHODS

RNase protection assay

Timed pregnant NIH Swiss females and adult mice were purchased from NCI Frederick. Gestational age of embryos [embryonic day (E) 0.5 defined by the presence of a vaginal plug the morning after mating] was confirmed by limb-bud development (Rugh, 1991). Bilateral gonads were dissected, the mesonephros removed (except for those at E11) and the tissue was frozen immediately on dry ice. The sex of the embryo was determined by detection of Zfy sequences in tail DNA (Nagamine et al., 1990) at E11 or by the presence of testis cords in older embryonic gonads. Gonads obtained from one- and two-week-old mice, and adult mice were processed in the same manner.

Total RNA was extracted with RNAzol-B (Tel-Tech) from gonads and the RNase protection assay was performed using the RPA III (Ambion) protocol. FIGα (1-759 bp) or ZP2 (22-743 bp) cDNA subcloned in BlueScript (Stratagene) was linearized with *Taq*I or *Dde*I, respectively. FIGα (333 nt, residues 478-759), ZP2 (204 nt, residues 552-743) and pTRI-actin-mouse (β-actin, 304 nt) antisense probes were labeled with [α-^{32}P]UTP (Amersham) using MAXIscript T7/T3 (Ambion) and gel purified according to the manufacturer's instructions. After linearization of the FIGα cDNA with *Not*I, full-length sense FIGα RNA was transcribed in the presence of excess cold NTPs and trace amounts of [α-^{3}H]CTP (NEN) to quantify the amount of synthetic RNA.

Optimal RNase digestion of hybridized probe and sample RNA was achieved by using RNase T1 (1:50 dilution). Standard curves for each experiment were obtained using known amounts (0.03-0.0001 fmole) of synthetic sense strand FIGα RNA. Yeast RNA, ovarian lysate or standards containing increasing amounts of the synthetic RNA were simultaneously hybridized with 0.4 fmole of ^{32}P-labeled antisense probe according to the manufacturer's instructions (DirectProtect Lysate RPA, Ambion). After RNase digestion, the protected fragments were separated on a 5% acrylamide-8 M urea gel and detected by autoradiography. The intensity of each band was determined using a PhosphorImager (Molecular Dynamics) and ImageQuant software. Results represented the average (±s.e.m.) of three to five independent experiments, each conducted with a standard curve.

RT-PCR

Newborn ovaries were isolated and frozen individually at –80°C prior to genotyping. RT-PCR was performed using total RNA, extracted with RNAzol (Tel-Tech), from pools (12-15) of FIGα null and normal ovaries. After treatment with Amplification Grade, DNase I (Life Technologies), RNA (0.5 μg) was primed with random hexamers (20 pmol) and reverse transcribed with Superscript™ First-Strand Synthesis System for RT-PCR according to the manufacturers instructions (Life Technologies). 10% of either normal or null cDNA was subjected to 35 cycles of PCR using the following conditions: 94°C for 30 seconds, 60°C for 30 seconds and 72°C for 1 minute. The following sense and antisense primers, respectively, were used for PCR (each is followed by the expected sizes of the PCR product): ZP1, 5′ CCAATGGCCGTGTGGAT and 5′ GGTGGTTGGGGTGA-GAAGA (826 bp); ZP2, 5′ GGGAAAACCCACCCTCCA and 5′ GCCACAGCACCCAGTGTT (730 bp); ZP3, 5′ GGCTCAGAGGG-TTGTCA and 5′ CGGGGATCTGGTTAGCT (661 bp); FIGα, 5′ ACTCCACCACGGATGACCTG and 5′ CTCGCACAGCTGGTAG-GTTGG (331 bp); and MSY2, 5′ GCACCATTGGAGGGTGATC-AACAGC and 5′ GATCCCTTCCTTCAACCCATGCTAG (509 bp). In addition, the presence of potential targets of FIGα, including integrins α6 and β1, KIT ligand, KIT receptor, connexin 43, fibroblast growth factor 8 (FGF8), growth differentiation factor 9 (GDF9), bone morphogenic protein 15 (BMP15) and E-cadherin was assayed by RT-PCR using published primers (Anderson et al., 1999) or primers based on sequence that yielded PCR products of expected sizes (available on request). RT/PCR assays were performed three times using independent pools of null and normal RNA as template and the absence of reverse transcriptase as a negative control.

In situ hybridization

Gonads from E15 (mesonephros intact) and E17 (mesonephros removed) embryos were fixed (ethanol:acetic acid::3:1, 1 hour, 20°C), and rinsed with 100%, 95% and 70% ethanol. Fixed tissue was embedded in paraffin and 6 μm sections were placed on silanated slides (Manova et al., 1990). To localize germ cells, sections were incubated (1 hour, 33°C) in a humid chamber with undiluted GCNA1 monoclonal hybridoma (rat IgM) supernatant (Enders and May, 1994), rinsed in TBS and incubated (1 hour, 20°C) with a goat anti-rat streptavidin conjugated second antibody (1:100). After detection with the ABC kit (Vector Labs), the sections were viewed by light microscopy and photographed.

A fragment of FIGα cDNA (333 bp, residues 478-759) was subcloned into Bluescript (Stratagene) and after linearization, sense and antisense labeled transcripts were generated using MAXIscript T7/T3 (Ambion) according to the manufacturer's specifications. Synthesis reactions were optimized (overnight, 4°C) for full-length transcripts using 80 pmoles of [α-^{33}P]UTP (Amersham) and 1 μg of the appropriate linearized template. The probes were purified on G-50 Sephadex mini-columns (5 PRIME → 3 PRIME). Prior to in situ hybridization (Epifano et al., 1995), ovarian and testis sections were digested (15 minutes, 37°C) with proteinase K (10 and 1 μg/ml, respectively). All slides were prehybridized (1 hour, 55°C) and then hybridized (16 hours, 55°C) with RNA probes (5×10^4 cpm/μl). The slides were dipped in Kodak NTB-2 emulsion, exposed for 21 days prior to development with Kodak Developer D-19 and counterstained with Hematoxylin (Fisher). Multiple slides of gonads from each sex were examined.

Generation of *Figα* mutant mice

1.8×10^6 bacteriophage of a lambda 129Sv mouse genomic library (Stratagene) were screened by plaque hybridization (Sambrook et al., 1989) with a ^{32}P-labeled mouse FIGα cDNA (Liang et al., 1997). Phage DNA was isolated, digested with *Not*I and the approx. 20 kbp insert subcloned into SuperCos 1 cosmid (Stratagene). Cosmid DNA was amplified in XL1-Blue MR cells (Stratagene) grown overnight at 30°C (LB broth, 50 μg/ml ampicillin) and purified with a Plasmid Maxi Kit (Qiagen). The sequence of the *Figα* locus was determined by DMSO-modified dideoxy-chain termination (Seto, 1990) using [α-^{35}S]dATP (Amersham) and the Sequenase Sequencing Kit (US Biochemicals, Version 2.0). Both strands of the coding regions were sequenced and the boundaries of exons were determined by comparison of the genomic sequence with that of FIGα cDNA (Liang et al., 1997). The sizes of introns were determined by DNA sequencing or polymerase chain reaction in a Perkin Elmer GeneAmp PCR System 9600 using *Figα* exon-specific forward and reverse oligonucleotide primers using 35 cycles of 95°C for 30 seconds, 55°C for 45 seconds and 72°C for 2 minutes. The first cycle was preceded by 5 minutes at 94°C and the last cycle was followed by a 7 minutes extension at 72°C. The PCR products were analyzed by agarose gel electrophoresis.

The *Figα* targeting construct was assembled sequentially in the pPNT vector (Tybulewicz et al., 1991) with a 1.6 kbp *Bsp*120I/*Hin*dIII fragment (extending from the middle of exon 1 into the beginning of intron 2) blunt-end ligated into the unique *Eco*RI site located between the PGK-Neo and PGK-TK cassettes and a 3.5 kbp *Xho*I *Figα* promoter fragment cloned 5′ to the PGK-Neo cassette. The plasmid was linearized with *Not*I and after electroporation into RI embryonic stem cells (Nagy et al., 1993), individual clones were selected by growth in G418 (Gibco) and gancyclovir (Roche Discovery). Cell lines with correctly targeted *Figα* alleles were identified by Southern blot analysis of *Eco*RI digested genomic DNA using ^{32}P-labeled 5′ (0.8 kbp *Ava*I fragment) and 3′ (0.6 kbp *Hin*dIII fragment) probes that detected 14 and 10 kbp fragments from the normal allele, respectively,

and a 24 kbp *Eco*RI fragment from the null allele. Identity of the mutant allele was confirmed by hybridization with a ^{32}P-labeled 0.6 kbp *Pst*I fragment isolated from PGK-Neo.

Heterozygous *Figα*$^{+/tm}$ cells from targeted cell lines were injected into C57BL/6N blastocysts to obtain coat color chimeras and germ line transmission was assayed by Southern blot analysis of DNA isolated from tails (Rankin et al., 1996). Founder chimeras were bred to females of the 129/SvJ.Jae and CF-1 strains. No histological differences of *Figα* null mutations were noted between strains and mice used for remaining analyses were maintained on a CF-1 background.

Histology and immunohistochemistry

Mullerian structures and gonads were dissected, placed in PBS and photographed immediately under a dissecting microscope. Gonads isolated from *Figα*$^{tm/tm}$ and normal mice were fixed (3 hours) in 3% glutaraldehyde in 0.1 M sodium cacodylate buffer, pH 7.2, rinsed in the same buffer without fixative and transferred to 70% ethanol. Tissues were dehydrated and embedded in methacrylate and 2 μm sections cut (American Histolabs). Mounted sections were stained with periodic-acid Schiff's reagent (PAS), counterstained with Hematoxylin and viewed by light microscopy for photography.

For immunohistochemistry, gonads were fixed in Bouin's solution (1-3 hours, 20°C) and rehydrated by briefly rinsing in PBS and then several times in 70% ethanol. After embedding in paraffin, 5 μm sections were affixed to silanated slides (Paragon Biotech, Inc). Sections were incubated (1 hour, 33°C) with undiluted GCNA1 monoclonal hybridoma (rat IgM) supernatant (a gift from Dr George Enders, University of Kansas, USA) that was then removed and replaced with FRGY2/MSY2 antibody (a gift from Dr Alan Wolffe, NIH, USA) for 16 hours, 4°C (Tafuri and Wolffe, 1990; Enders and May, 1994; Gu et al., 1998). Sections were rinsed three times in TBS. Two fluorescent secondary antibodies, CY5-conjugated goat anti-rabbit IgG (Jackson Immunoresearch) and Oregon Green 488 conjugated goat anti-rat IgG (Molecular Probes) were added sequentially to detect MSY2 and GCNA1, respectively, by confocal microscopy (Zeiss LSM 5 Laser Scanning Confocal Microscope).

RESULTS

Embryonic expression of *Figα*

FIGα transcripts were not detected in the female urogenital ridges at E11 by which time many migrating germ cells have colonized the gonad. Low levels of FIGα transcripts were first observed at E13, shortly after the onset of sexual dimorphism of the gonads, when female germ cells begin to enter into the prophase of meiosis I (MI; Fig. 1A, top). Transcript abundance dramatically increased at the end of embryonic development and peaked approximately two days post partum (dpp) (Fig. 1A,B), a time in ovarian development at which oocytes have become enclosed in primordial follicles. However, even at peak abundance (2 dpp), FIGα transcripts were present at only 350 zeptomoles per gonad (Fig. 1B).

FIGα mRNA levels decreased markedly by 7 and 14 days after birth and transcripts were barely detectable in adult ovaries using β-actin mRNA as a load control and for assessment of RNA integrity. Although the number of germ cells declines after birth, much of the postnatal decrease in abundance reflected a dilutional effect of RNA contributed by proliferating somatic cells and FIGα transcripts persist in oocytes of adult ovaries (Liang et al., 1997). Using this RNase protection assay, FIGα transcripts were not detected in male embryos (Fig. 1A, bottom), although low levels of FIGα transcripts and protein have been observed in testes from adult males (Liang et al., 1997; Millar et al., 1991) and transcripts can be detected in embryonic testes by RT-PCR (data not shown).

To determine the cellular specificity of *Figα* expression during embryonic development, E15 urogenital ridges and E17 gonads were examined by in situ hybridization. The E15 urogenital ridge is composed of the gonad and the mesonephros, an anlage of the developing kidney (Fig. 2B). The presence of germ cells within the gonad was ascertained using an antibody specific to GCNA1, germ cell nuclear antigen 1 (Fig. 2A). Even at initial stages of expression (E15), FIGα transcripts were restricted to the cytoplasm of cells (Fig. 2C,D) that aligned to oocytes in serial sections stained with GCNA1 (Fig. 2A) or Hematoxylin and Eosin (Fig. 2B). At E17 FIGα transcripts were clearly restricted to oocytes within the ovary (Fig. 2E) and ^{33}P-labeled sense controls (Fig. 2F) gave signals that were no greater than those observed over the mesonephros lacking germ cells (Fig. 2C). As anticipated by the absence of FIGα transcripts in male gonads (Fig. 1A), no signals greater than background were observed in male gonads (data not shown).

Targeted mutagenesis of *Figα*

A 129/Sv mouse genomic library was screened with full-length FIGα cDNA to isolate a clone with a approx. 20 kbp fragment containing the *Figα* gene locus. The *Figα* gene was characterized by DNA sequencing and PCR (Fig. 3A, top). Three exons (267 bp, 200 bp, >130 bp) were identified that encoded the 194 amino acid FIGα protein. The first and second introns were approx. 1100 bp and 2130 bp, respectively. The *Figα* targeting construct (Fig. 3A, middle), containing 5.2 kbp of isogenic DNA (3.5 kbp 5′ to the transcription start site and 1.6 kbp including portions of the first two exons) was designed to delete the transcription and translation start sites. After electroporation into RI embryonic stem cells, 1.7% of 300 cell lines isolated after positive-negative selection (Thomas and Capecchi, 1987) were successfully targeted (Fig. 3B). Of the five independently targeted cell lines, two were injected into C57BL/6 host blastocysts to derive mouse lines. Coat color chimera were bred to CF-1 females to obtain F_1 heterozygotes. Both male and female F_1 heterozygotes were fertile and, when mated, produced F_2 normal, heterozygous (+/tm) and homozygous(tm/tm) null mutant offspring in the expected Mendelian ratios for a mutation in a single-copy gene (Fig. 3C). To ensure that *Figα* expression was absent in null mice, total ovarian RNA was extracted from heterozygous and homozygous *Figα* null E19 female mice and analyzed by RNase protection (Fig. 7A). *Figα* was expressed in heterozygous (+/tm), but not in homozygous (tm/tm) null ovaries, confirming the inactivation of the gene. The presence of β-actin in both samples assured the integrity of the RNA and served as a load control. Two independently derived mouse lines with germline transmission, *Figα*$^{tm1Nih/tm1Nih}$ and *Figα*$^{tm2Nih/tm2Nih}$ have been stably maintained for over 2 years.

Sexually dimorphic effects on *Figla* null gonads and fertility

Figα null mice appeared normal at birth, grew to adulthood and both sexes (6 weeks old) exhibited normal mating behavior and evidence of copulation. Fertility was assessed after

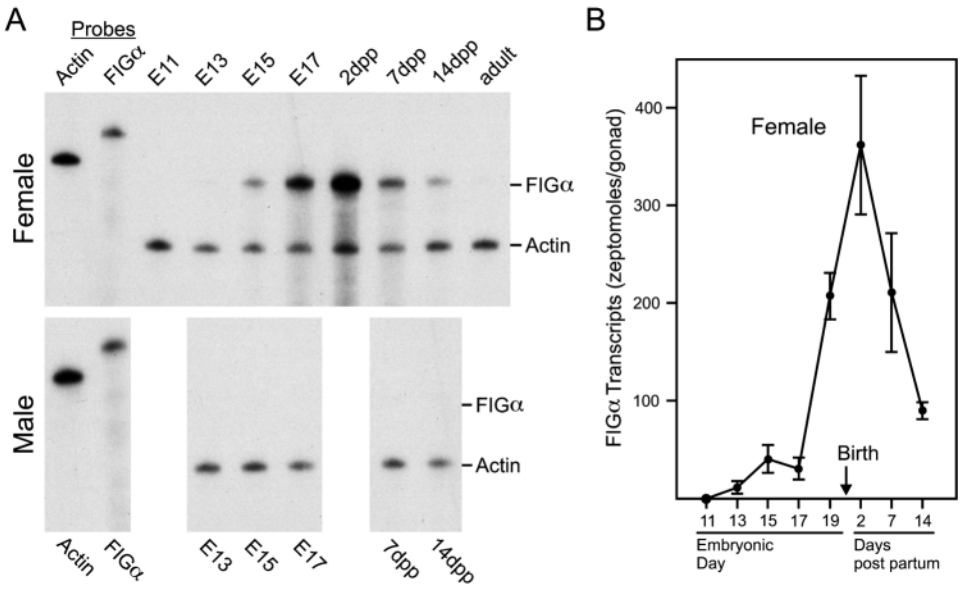

Fig. 1. Developmental expression of *Figα* mRNA during gonadogenesis. (A) The abundance of FIGα transcripts was determined with an RNase protection assay using ^{32}P-labeled antisense probes specific for FIGα (333 nt) and β-actin (304 nt). Total RNA (5 μg) was extracted from ovaries or testes isolated from E11, E13, E15 and E17 or post partum (2 dpp, 7 dpp, 14 dpp, adult) mice. After RNase digestion, protected fragments (FIGα, 299 nt; β-actin, 250 nt) were detected by autoradiography. (B) The accumulation of FIGα transcripts was determined by comparing the signals obtained from developmentally staged gonads with those obtained (data not shown) in identical assays using increasing amounts of synthetic FIGα transcripts. The values (zeptomoles) on the ordinate were obtained by a phosphorimager and represent the average of three to five experiments (±s.e.m.) expressed per gonad.

breeding normal, heterozygous and homozygous *Figα* null mice with one another (Table I). When compared with normal matings (8.8±0.2 pups), homozygous *Figα* null male mice (*Figα*$^{tm/tm}$) had normal fertility when mated with normal (10.1±0.6 pups) or heterozygous (9.0±1.4 pups) *Figα* null females. Likewise, female heterozygotes (*Figα*$^{+/tm}$) mated with normal males gave birth at the same time and with the same litter sizes (9.0±1.5 pups) as normal females. In contrast, homozygous null females (9) mated with normal males did not become visibly pregnant and produced no litters. The production of litters from age- matched females co-caged with the *Figα*$^{tm/tm}$ females assured the continued fertility of the stud male.

To investigate the cause of the observed female sterility, reproductive tracts were dissected from normal, heterozygous and homozygous null littermates at 6 weeks of age. Mullerian structures (oviduct, uterus, upper vagina) were present in *Figα* homozygous null mice, but the size of their ovaries was one-twentieth of that observed in normal and heterozygous *Figα* null littermates (Fig. 4A). Histologically, the shrunken *Figα* null ovaries were devoid of oocytes or follicles and contained only cord-like clusters of stromal cells (Fig. 4B). In contrast, the age-matched normal ovaries contained active follicles at various stages of growth as well as corpora lutea that are indicative of past ovulations (Fig. 4C).

No differences were observed in comparing the reproductive tracts of homozygous *Figα* null male mice to heterozygotes or normal controls. The testes were grossly indistinguishable among the three genotypes (Fig. 4D) and the architecture of seminiferous tubules in the *Figα* null was normal with the presence of primary and secondary spermatocytes as well as maturing spermatozoa in the lumen. There also appeared to be a normal complement of somatic lineages including Sertoli, Leydig and myoid cells (Fig. 5E,F). Mature sperm, dissected from the epididymides, were motile and their numbers did not deviate grossly from that observed in normals. Null males had normal fertility (Table 1) and thus, if there is a phenotype in homozygous *Figα* null males, it must be subtle.

Primordial follicles do not form in *Figα* null females and germ cells disappear after birth

The detection of FIGα transcripts beginning at embryonic day 13 suggested that the sterile phenotype observed in adult null females arose at a much earlier time in development. Therefore, ovaries were dissected from null mice at E15.5 and E18 for comparison to normal gonads. Histologically they appeared very similar. Both null and normal ovaries at E18 were filled with germ cells (Fig. 5A-D) and there was morphological evidence of progression into the prophase of meiosis I with apparent condensation of chromatids (Fig. 5C,D). The null phenotype began to evolve in the newborn ovary (Fig. 5E-H) and was quite dramatic by 1 day after birth (Fig. 5I-L). Normal folliculogenesis is initiated by growth of oocytes in the medullary region where somatic cells begin to adhere to germ cells (Fig. 5F,H) and by one day after birth primordial follicles have formed (Fig. 5J,L). However, in *Figα*

Table 1. Number of live births

	Male parent		
Female parent	Normal (*Figα*$^{+/+}$)	Heterozygous (*Figα*$^{+/tm}$)	Homozygous (*Figα*$^{tm/tm}$)
Normal (*Figα*$^{+/+}$)	8.8±0.2 (5)*	9.2±1.3 (5)	10.1±0.6 (7)
Heterozygous (*Figα*$^{+/tm}$)	9.0±1.5 (6)	10.8±0.4 (8)	9.0±1.4 (5)
Homozygous (*Figα*$^{tm/tm}$)	0 (0)	nm	0 (0)

*Mean±s.e.m. (number of litters) of at least five mating pairs.
nm, not mated.

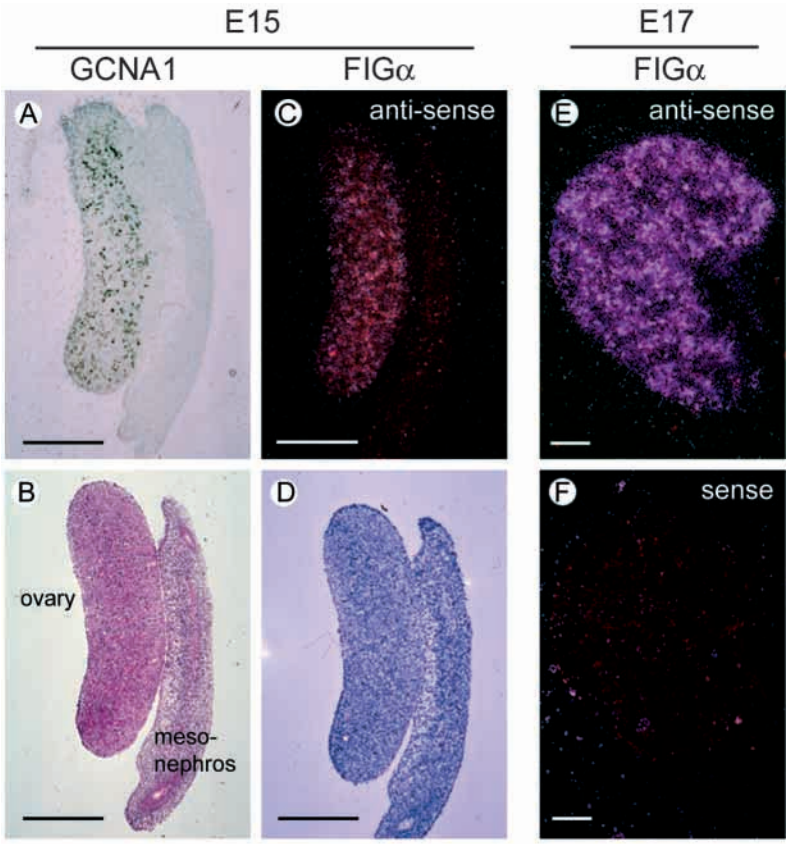

Fig. 2. Localization of FIGα transcripts in embryonic mouse ovaries. (A) Serial sections of paraffin-embedded E15 urogenital ridges (gonad and mesonephros) were stained with a rat monoclonal antibody specific to GCNA1 (Enders and May, 1994) and (B) with Hematoxylin and eosin to localize germ cells within the ovary. Antibody binding in the nucleus of oocytes was detected with an alkaline phosphatase conjugated goat anti-rat secondary antibody. (C) Ovarian sections isolated from E15 and from E17 embryos (E) were hybridized in situ with ^{33}P-labeled antisense FIGα probes and viewed under dark field. FIGα transcripts were present only in the gonad of the urogenital ridge and were restricted to oocytes within E15 and E17 ovaries. (D) Serial bright-field images helped to localize the germ cells within the ovary (E15). (F) Hybridization of sections with ^{33}P-labeled sense served as negative controls (E17). Scale bars, 250 μm.

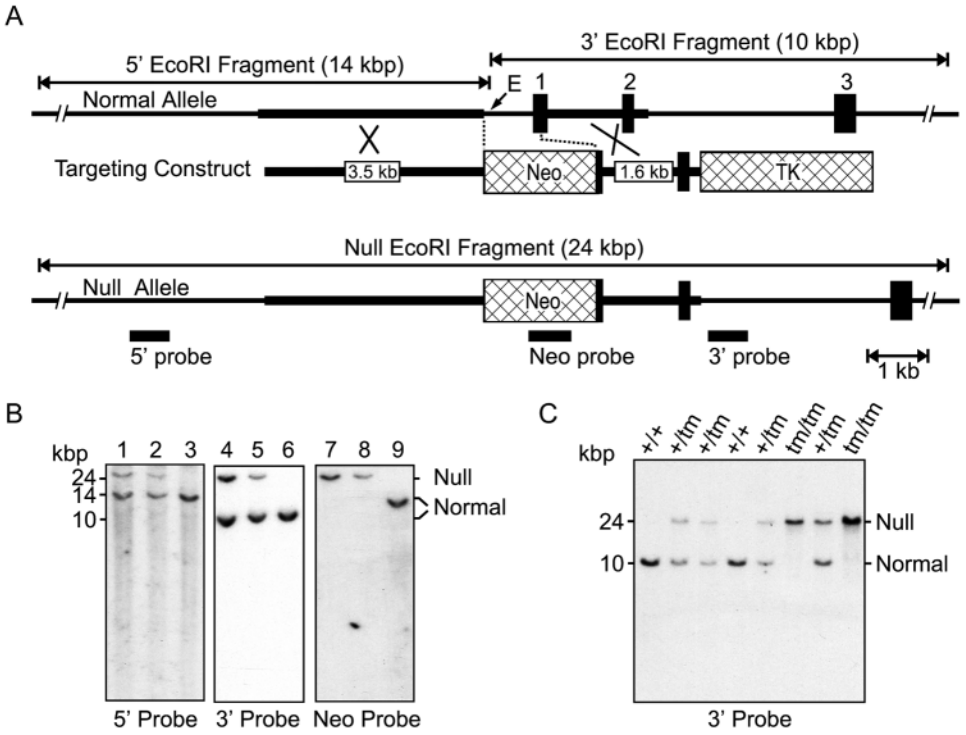

Fig. 3. Generation of mouse lines lacking FIGα. (A) Top, schematic representation of the normal *Figα* allele with three exons. Middle, the targeting construct with PGK-Neo and PGK-TK as positive and negative selectable markers respectively, was designed to delete 0.8 kbp of *Figα* that included the transcriptional and translational start sites. Homologous regions include 3.5 kbp in the promoter and 1.6 kbp that encompasses exon 2 and half of exon 1. Bottom, the *Figα* allele mutated by homologous recombination. Vertical boxes represent exons; *Eco*RI fragments are indicated above the normal and null alleles; thicker lines indicate extent of homologous DNA; and positions of the 5′ probe, 3′ probe and neo probe are indicated under the null allele. (B) Genotyping of embryonic stem cells by Southern blot analysis of purified DNA hybridized with ^{32}P-labeled 5′ (left), 3′ (middle) and neo (right) probes. After digestion with *Eco*RI, the normal and mutant alleles detected with the 5′ probe had restriction enzyme fragments of 14 and 24 kbp, respectively, and the normal and mutant alleles detected with either the 3′ or neo probes had restriction enzyme fragments of 10 and 24 kbp, respectively. Lanes 1,4,7 and 2,5,8 represent two targeted RI cell lines; lanes 3,6,9 represent a line not correctly targeted. (C) Genotyping by Southern blot analysis of DNA purified from tails of F_2 females generated from a $Fig\alpha^{+/tm} \times Fig\alpha^{+/tm}$ cross after restriction digest with *Eco*RI and hybridization with the ^{32}P-labeled 3′ probe. Normal (+/+), heterozygous (+/tm) and homozygous (tm/tm) *Figα* null genotypes were present in the expected mendelian ratios of a single copy mutant gene.

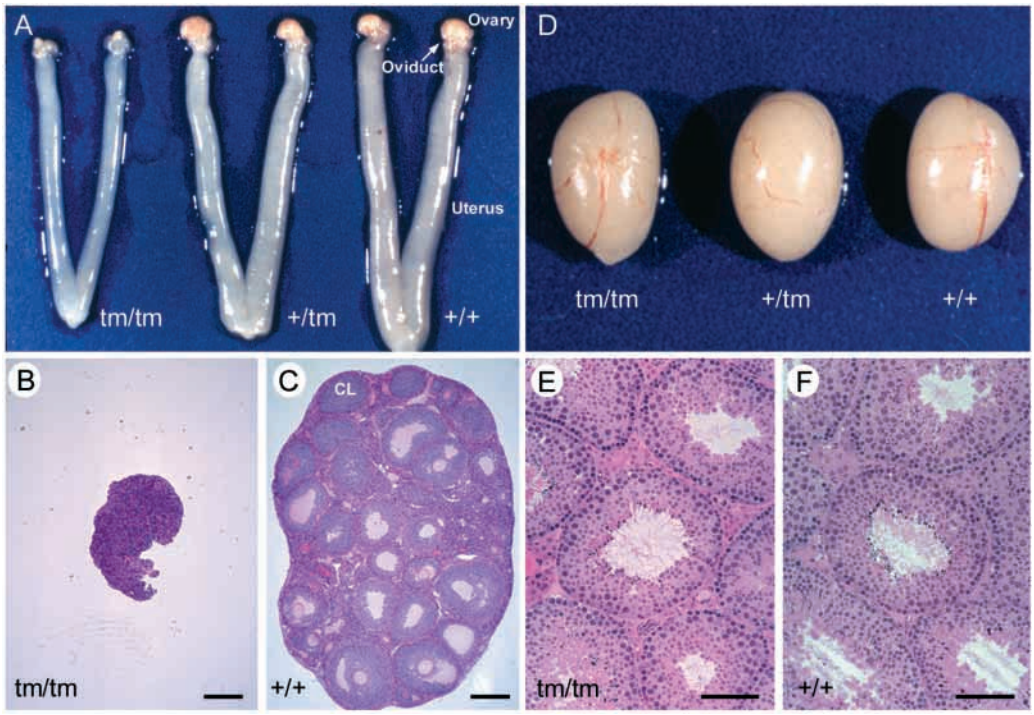

Fig. 4. Morphology and histology of adult gonads. (A) Although thinner and somewhat atrophic, the Mullerian-derived structures (uterus, oviducts) of 6-week-old homozygous *Figα* null (tm/tm) mice appear similar to those obtained from heterozygous (+/tm) and normal (+/+) mice. However, ovaries from homozygous *Figα* null mice, shown resting on the oviducts (A), are one-twentieth the size (midline cross sectional area) of normal or heterozygous null ovaries. (B) Histological sections of *Figα* null ovaries fixed in 3% glutaraldehyde and stained with periodic-acid Schiff's reagent and Hematoxylin confirmed the small size of the *Figα* null ovaries and demonstrated a total absence of follicles and germ cells. (C) Histology of an ovary from a normal littermate with normal folliculogenesis including corpora lutea (CL) indicative of past ovulations and a normal complement of germ cells. (D) The size and appearance of the *Figα* null (tm/tm) testes were indistinguishable from heterozygous (+/tm) normal (+/+) testes. (E,F) The architecture of the *Figα* null seminiferous tubules appeared normal with the presence of primary, secondary and mature spermatozoa within the lumen as well as a normal complement of supporting cells (Sertoli within the seminiferous tubules and Leydig and myoid within the interstitium). Scale bars, 250 μm in B,C; 100 μm in E,F.

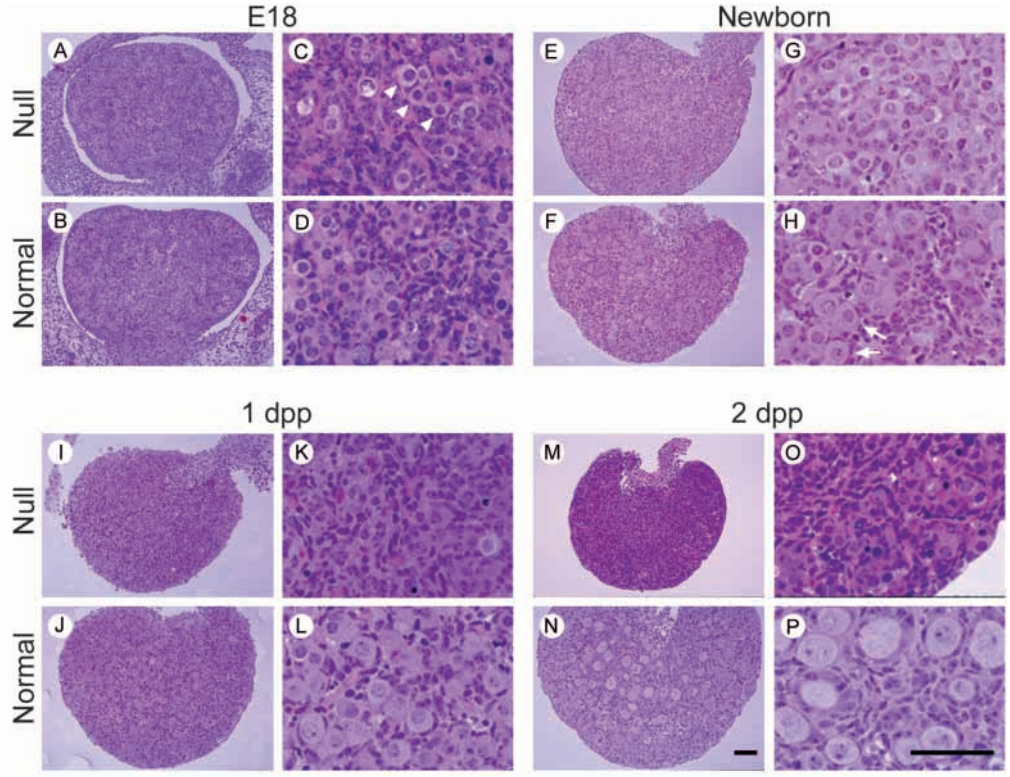

Fig. 5. Histological comparison of folliculogenesis in normal and null ovaries. Ovaries were dissected from *Figα* normal (+/+) and null (tm/tm) littermates at E18 (A-D), newborn (E-H), 1 dpp (I-L) and 2 dpp (M-P). Formaldehyde fixed, plastic-embedded ovaries were sectioned and stained with periodic-acid Schiff's reagents and Hematoxylin. Low and high magnification images were paired (A,C; B,D; E,G; F,H; I,K; J,L; M,O; N,P) and scale bars (25 μm) for each are in panels (N) and (P), respectively. Ovaries from E18 null (A,C) and normal (B,D) mice had similar numbers of germ cells (arrowheads) clustered within intervening stromal cells. Although many oocytes were still present in *Figα* null newborn ovaries (E,G), they remained in clusters and follicular cells did not adhere to them to form primordial follicles as they did with oocytes in the medulla of normal ovaries (F,H, arrows). By 1 dpp, most non-follicle-enclosed oocytes in the central region of the null ovaries had disappeared (I,K), whereas there were many well-separated primordial follicles in normal ovaries (J,L). By 2 dpp, only a few cortical oocytes remained in *Figα* null ovaries (M,O), and the absence of germ cells accounted for the smaller size of the gonad. In contrast, ovaries from normal littermates (N,P) contained numerous primordial follicles, some of which had already begun to grow.

null mice the diameter of oocytes did not increase in newborn ovaries, somatic cells did not adhere to and surround germ cells (Fig. 5E,G), and oocytes had begun to disappear by 1 day after birth (Fig. 5I,K). Normally, by 2 days after birth, oocytes have formed well-defined primordial follicles in which the 12-15 μm diameter germ cells are surrounded by a single layer of flattened granulosa cells and contained within an outer basal lamina (Fig. 5N,P). These represent the entire complement of germ cells (10,000-15,000) available to the female and serve as a pool from which cohorts will be selected for growth and ovulation. In stark contrast to the normal ovary, no primordial follicles were present in shrunken *Figα* null ovaries which were massively depleted of germ cells (Fig. 5M,O). The few scattered oocytes that remained in the periphery of the gonad (Fig. 5O) completely disappeared by 7 days after birth (data not shown). The residual cells formed cord-like structures that became more evident in older *Figα* null females.

Oocyte-granulosa cell interactions are important for normal folliculogenesis (Eppig et al., 1997) and ectopic germ cells not enclosed in granulosa cells do not survive beyond 2-3 weeks (Zamboni and Upadhyay, 1983). A number of cell surface proteins (e.g. E-cadherin, connexin43, KIT receptor, KIT ligand, α6 and β1 integrins) and growth factors (e.g. GDF9, BMP15, FGF8) have been implicated in early ovarian folliculogenesis (Valve et al., 1997; Elvin and Matzuk, 1998; Juneja et al., 1999; Mackay et al., 1999; Dube et al., 1998). Therefore, RT-PCR was used to determine if transcripts of the aforementioned macromolecules were present in *Figα* null ovaries. RNA was isolated from newborn ovaries and random-primed cDNA was used as a template for PCR with synthetic oligonucleotides specific to E-cadherin, connexin43, KIT receptor, KIT ligand, the subunits of α6 and β1 integrins, GDF-9, BMP-15 and FGF-8. PCR products for each transcript were detected in both normal and *Figα* null ovaries and control reactions lacking reverse transcriptase were uniformly negative (data not shown). Thus, the inability of *Figα* null mice to form primordial follicles does not appear to result from an absence of transcripts encoding these proteins, although quantitative difference or oocyte-specific absence could contribute to the observed phenotype.

Figα null mice progress through the prophase of the first meiotic division

The phenotype in *Figα* null female mice was reminiscent of that observed in induced mutations of factors required for progression of germ cells through the pachytene stage of MI (Yoshida et al., 1998; Pittman et al., 1998; Barlow et al., 1998; de Vries et al., 1999; Edelmann et al., 1999). Therefore, immunohistochemistry was performed with antibodies that distinguish specific meiotic stages of oocyte development. GCNA1 (a nuclear protein of unknown function), is expressed by primordial germ cells as they colonize the gonad at E11.5 and continues to be detected as oocytes enter into meiosis and progress through leptotene, zygotene and pachytene stages of the prophase of MI. The antigen is not observed in the diplotene or the dictyate, an arrested state unique to oocytes that persists from shortly after birth until just prior to ovulation (Enders and May, 1994). In a complementary fashion, the oocyte-specific, cytoplasmic RNA-binding protein, MSY2 is not expressed in the early stages of prophase I, but only after oocytes have entered into the diplotene. This protein persists in the dicytate, a period of abundant transcription and storage of newly synthesized transcripts into RNPs (Gu et al., 1998).

Antibodies to each marker were added concurrently to ovarian sections and imaged by laser confocal microscopy using fluorescent secondary antibodies that distinguished between GCNA1 (green) and MSY2 (red) primary antibodies (Fig. 6, top). In E19 (Fig. 6A,B) and newborn (Fig. 6C,D) ovaries, comparable numbers of null and normal oocytes had reached the pachytene and diplotene stages of MI prophase. However, beginning with newborns, there was an apparent decrease in the number of diplotene stage oocytes in *Figα* null

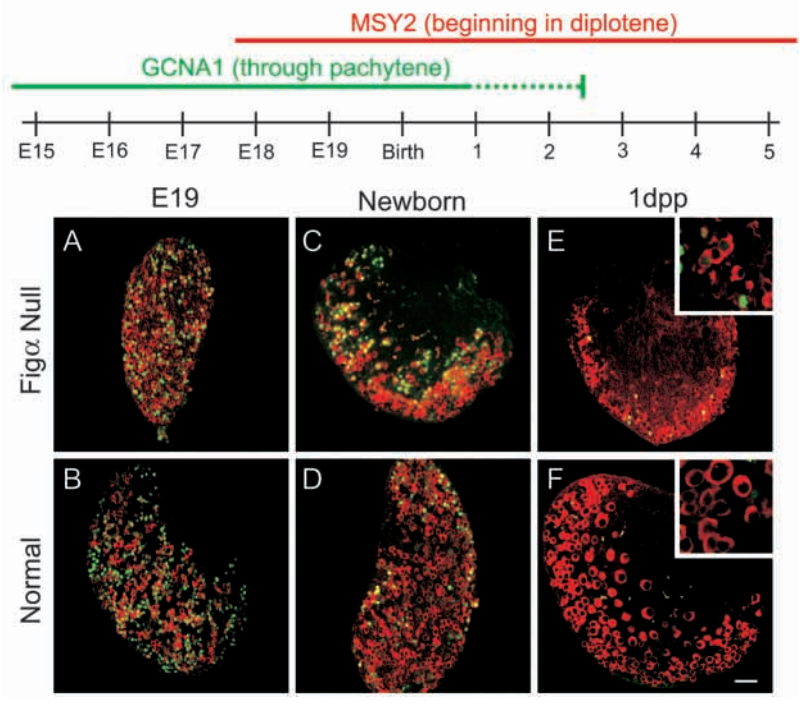

Fig. 6. Analysis of meiotic progression in pre- and perinatal ovaries. Progression through the prophase of the first meiotic division was detected using antibodies to two stage-specific markers: GCNA1, expressed in nuclei of germ cells from the time they colonize the genital ridge until the end of the pachytene stage of meiosis I (Enders and May, 1994); and MSY2, a cytoplasmic Y box protein expressed in oocytes that have reached the diplotene stage of meiosis I (Gu et al., 1998). Ovaries from fetal and newborn ovaries were fixed in Bouin's, embedded in paraffin and stained consecutively with antibodies to GCNA1 and MSY2. Using laser confocal microscopy, the binding of primary antibodies to MSY2 and GCNA1 was detected by CY^{TM}5-conjugated goat anti-rabbit IgG (H+L) and Oregon Green^{R} 488 goat anti-rat IgG (H+L) conjugate, respectively. At E19 and in newborns, both meiotic markers were present in *Figα* null (A,C) and normal (B,D) oocytes, indicative of meiotic progression from the pachytene (green) to diplotene (red) stages. (E) At 1 dpp, a few pachytene oocytes were still detected at the periphery of null ovaries but the loss of diplotene oocytes was much more marked. Conversely, virtually all oocytes had reached the diplotene stage in normal mice at 1 dpp (F). Insets show oocytes at higher magnification to highlight the growth of some oocytes in the normal, but not in the null 1 dpp ovaries. Scale bar, 25 μm.

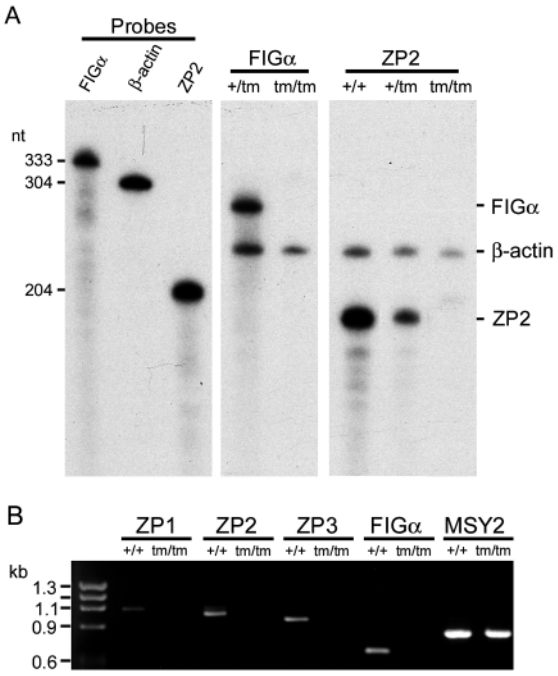

Fig. 7. *Figα* null mice do not express zona genes. (A) RNase protection assay of FIGα and ZP2 transcripts in E19 ovaries. Left panel, ^{32}P-labeled antisense FIGα (333 nt), β-actin (304 nt) and ZP2 (204 nt) probes. Total RNA (5 μg) from normal (+/+), heterozygous (+/tm) and homozygous (tm/tm) *Figα* null mice was assayed with the FIGα and β-actin (middle panel) or ZP2 and β-actin (right panel) ^{32}P-labeled probes. Protected FIGα (299 nt), β-actin (250 nt) and ZP2 (192 nt) fragments were detected after RNase digestion and autoradiography. (B) RT-PCR assay for ZP1, ZP2 and ZP3 transcripts in newborn ovaries isolated from normal (+/+) and *Figα* null (tm/tm) mice. Random hexamer primed RNA was used to make cDNA from total RNA and synthetic oligonucleotides specific to each transcript were used in PCR to detect ZP1 (826 bp), ZP2 (730 bp) and ZP3 (661 bp). The presence of MSY2 (509 bp) and the absence FIGα (331 bp) RT-PCR products in homozygous null mice provided positive and negative controls, respectively. No PCR signals were observed in the absence of reverse transcriptase.

ovaries (Fig. 6C,D), although clearly progression through the prophase of MI was possible as evident by the presence of the MSY2 (red) marker. The loss of diplotene stage oocytes was more marked at 1 day after birth (Fig. 6E) in *Figα* null mice. At the same point in time, almost all of the oocytes in the normal ovary had progressed to the diplotene stage (Fig. 6F) where they arrested in dictyate. A number of the normal, but none of the *Figα* null oocytes had begun to grow by one day after birth (Fig. 6E,F, insets).

Female mice lacking FIGα do not express the zona genes

Earlier transactivation assays in heterologous cells using reporter genes coupled to zona promoters indicated that FIGα binds as a heterodimer (FIGα/E12) to an E box upstream of *Zp1*, *Zp2* and *Zp3*. These studies provided in vitro evidence that this protein-DNA interaction is necessary (but not sufficient) for zona gene expression (Liang et al., 1997). To confirm these observations in vivo, the presence of zona transcripts was assayed in normal, heterozygous and homozygous *Figα* null embryonic ovaries using an RNase protection assay. Earlier investigations had indicated that ZP2 transcripts were present earlier in oogenesis and in greater abundance than ZP1 and ZP3 transcripts (Epifano et al., 1995). In the current assay, ZP2 (but not ZP3, data not shown) transcripts were detected in normal (+/+) and heterozygous (+/tm) *Figα* null ovaries at E19 (Fig. 7A, right), a developmental time at which FIGα transcripts were also present (Fig.7A, middle, lane 1). The observation that there were no ZP2 transcripts in homozygous (tm/tm) *Figα* null mice at E19 (Fig. 7A, right panel, lane 3, even after longer exposure) confirmed an epistatic relationship between the two genes with *Figα* acting upstream of *Zp2*. These observations were extended using a more sensitive RT-PCR assay in which all three zona transcripts were detected in neonatal ovaries isolated from normal (+/+) mice. However, in the absence of FIGα, none of the zona transcripts (ZP1, ZP2, ZP3) was detected in ovaries isolated from homozygous (tm/tm) *Figα* null mice (Fig. 7B). The absence of FIGα transcripts and the presence of MSY2 transcripts in the null ovaries, served as

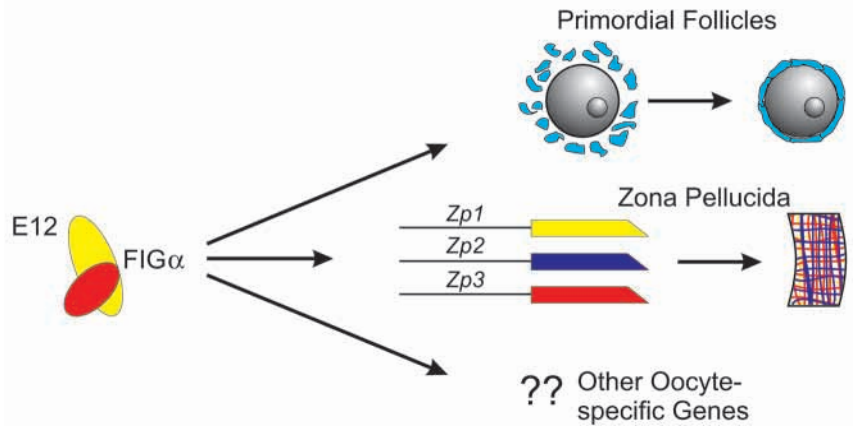

Fig. 8. Multiple targets for FIGα. FIGα heterodimerizes with E12, a ubiquitous bHLH protein, and binds upstream of one or more genes, the expression of which is required for primordial follicle formation. In addition, FIGα is required for the expression of the three zona pellucida genes (*Zp1*, *Zp2* and *Zp3*), without which the zona matrix is not formed. The persistence of FIGα in oocytes from embryonic day 13 until they are fully grown suggests that FIGα may modulate additional genes that are important for normal oogenesis and early development.

negative and positive controls, respectively. No PCR products were observed in the absence of reverse transcriptase (data not shown). Taken together with earlier in vitro binding data, these results are consistent with a model in which FIGα is required for zona gene expression. Thus, at a minimum, FIGα regulates two independent developmental processes, formation of primordial follicles and formation of the zona pellucida. Its persistence in adult oocytes also suggests additional roles (Fig. 8).

DISCUSSION

Germ cells are the only cells that contribute to the next generation and there is considerable evidence that they play an active role in ensuring the success of this endeavor through specific gene expression. FIGα is the first germ cell-specific transcription factor shown to affect mouse folliculogenesis in vivo and the absence of primordial follicles in *Figα* null mice establishes its requirement for the earliest interactions between oocytes and granulosa cells. *Figα* encodes a 194 amino acid (21 kDa) bHLH protein (Liang et al., 1997) and such transcription factors have been implicated in tissue-specific regulation of a wide range of genes (Littlewood, 1998). Most commonly, they bind to promoters as heterodimers with one component fairly ubiquitously expressed (e.g. E2A, E2-2, HEB) and the other expressed only in the tissue associated with the target genes (e.g. MyoD, for review see Olson and Klein, 1998). Structural studies indicate a critical role for the helix-loop-helix domain both in forming the duplex and in binding to DNA. The amino acid residues in the basic regions form contacts with nucleic acids in the major groove of the double helix. Although in vitro studies indicate that FIGα/E12 heterodimers can bind to E boxes in each of the three zona promoters, direct binding has not been demonstrated in vivo and recent observations that SCL (stem cell leukemia factor), a bHLH factor required for hematopoietic and vascular development, affects expression without DNA binding suggests other possible mechanisms of action (Porcher et al., 1999).

Normally, as oocytes transit from pachytene to diplotene prior to arresting in the dictyate shortly after birth, DNA-repair proteins and other factors are required for proper chromosome alignment and recombination. Germ cells from mice lacking MSH5 (homolog of bacterial MutS) and those that lack germline-specific DMC1 (homolog of RecA) or ATM, a post-synapsis surveillance protein, do not complete meiosis and are invariably lost from the ovary prior to diplotene (Yoshida et al., 1998; Pittman et al., 1998; Barlow et al., 1998; de Vries et al., 1999; Edelmann et al., 1999). The perinatal depletion of oocytes reported in these females is similar to that observed in *Figα* null mice. However, these phenotypes are recapitulated in male mice at the onset of meiosis which is delayed until more than a week after birth. Thus, the observation that adult *Figα* null males are fertile with normal testicular histology, and the morphological and biochemical evidence that female germ cells can progress through the prophase of MI, make it unlikely that the *Figα* phenotype is due to a defect in meiosis I. Given earlier observations that ectopically displaced germ cells that cannot participate in follicle formation do not survive beyond 1-2 weeks (Zamboni and Upadhyay, 1983), it seems more likely that the depletion of germ cells observed in *Figα* null mice and the resultant sterility arise from an inability of oocytes and granulosa cells to form primordial follicles. However, the downstream targets of FIGα required for primordial follicle formation remain to be determined. Although cell-surface adhesion molecules are attractive candidates, it has yet to be established whether FIGα affects only the oocytes in which it is expressed or if it induces the expression of factors that promote adhesion of somatic cells to germ cells. Alternatively, FIGα could modulate oocyte-specific growth/survival factors as the germ cell passes through diplotene to arrest in the dictyate, a pause in mouse meiosis that normally persists until ovulation.

The initial stage of folliculogenesis is independent of pituitary gonadotrophins and is thought primarily to involve intraovarian paracrine factors (Kol and Adashi, 1995). Transcripts encoding FGF8 are present in maturing oocytes (Valve et al., 1997), although the embryonic lethality of *Fgf8* null mutants have precluded a genetic analysis of its role in follicular growth. (Sun et al., 1999). In addition, three members of the transforming growth factor β (TGFβ) super family have been implicated in regulating early folliculogenesis. One, anti-Mullerian hormone (or Mullerian inhibiting substance) is expressed in granulosa cells surrounding oocytes and has been implicated in the recruitment of primordial follicles into the growth phase of folliculogenesis (Durlinger et al., 1999). Other members of the TGFβ family, BMP15 and GDF9, are first expressed in oocytes in primary follicles and persist in eggs even after ovulation (Dube et al., 1998; McGrath et al., 1995). Ovaries in female mice lacking GDF9 form primordial follicles, but do not progress beyond the primary follicle stage in which a single layer of cuboidal granulosa cells surrounds the growing oocyte. Some aspects of oogenesis proceed including growth and formation of a zona pellucida, but organelle structures are missing or altered, meiotic competence is impaired and females are sterile (Dong et al., 1996). However, primordial follicles are formed in *Gdf9* null mice which suggests that FIGα must regulate genes that function earlier in development, the absence of which precludes initial oocyte-granulosa cell interactions.

These results suggest that FIGα is a germ cell-specific bHLH transcription factor that plays key regulatory roles in preserving oocytes and in ensuring early embryo survival. Perinatally FIGα is required for primordial follicle formation without which oocytes are irretrievably lost from the newborn ovary. The inability of *Figα* null oocytes to interact with granulosa cells presumably results from abnormal expression of downstream gene(s) that may or may not act cell autonomously. Later in folliculogenesis, activation of the zona genes by FIGα leads to the secretion of three glycoproteins to form the zona pellucida, an extracellular egg coat that mediates fertilization and is required for passage of embryos through the oviduct (Rankin and Dean, 2000). Mice lacking FIGα do not express ZP1, ZP2 or ZP3 (this paper), and genetically altered mice not producing ZP1 or ZP3 have abnormal or absent zonae pellucidae with decreased fecundity or infertility, respectively (Rankin et al., 1996, 1999). Thus, at a minimum, FIGα regulates two sets of genes required for oocyte and early embryonic survival. The persistence of *Figα* expression from mid-gestation (E13) into adulthood suggests that FIGα may regulate other oocyte-specific genes as well.

We appreciate our instructive conversations with Drs John Eppig and Robert Scully on ovarian histology, and are grateful for the critical reading of the manuscript by Dr Eppig. We thank Drs Tracy Rankin and Eric Lee for their advice and help with the embryonic stem cells; Dr Li-fang Liang for the initial isolation of the *Figα* gene; Lyn Gold for help with embryonic manipulations; and Heidi Dorward for her confocal microscopy expertise.

REFERENCES

Anderson, R., Fassler, R., Georges-Labouesse, E., Hynes, R. O., Bader, B. L., Kreidberg, J. A., Schaible, K., Heasman, J. and Wylie, C. (1999). Mouse primordial germ cells lacking beta1 integrins enter the germline but fail to migrate normally to the gonads. *Development* **126**, 1655-1664.

Barlow, C., Liyanage, M., Moens, P. B., Tarsounas, M., Nagashima, K., Brown, K., Rottinghaus, S., Jackson, S. P., Tagle, D., Ried, T. and Wynshaw-Boris, A. (1998). Atm deficiency results in severe meiotic disruption as early as leptonema of prophase I. *Development* **125**, 4007-4017.

Brambell, F. W. R. (1928). The development and morphology of the gonads of the mouse. Part III. The growth of the follicles. *Proc. R. Soc. Lond. B Biol.* **103**, 258- 272.

Capel, B. (1998). Sex in the 90s: SRY and the switch to the male pathway. *Annu. Rev. Physiol.* **60**, 497-523.

Columbre, J. L. and Russell, E. S. (1954). Analysis of the pleiotrophism of the W-locus in the mouse: The effects of W and W^v substitution upon postnatal development of germ cells. *J. Exp. Zool.* **126**, 277-296.

de Vries, S. S., Baart, E. B., Dekker, M., Siezen, A., de Rooij, D. G., de Boer, P. and te Riele, H. (1999). Mouse MutS-like protein Msh5 is required for proper chromosome synapsis in male and female meiosis. *Genes Dev.* **13**, 523-531.

Dong, J., Albertini, D. F., Nishimori, K., Kumar, T. R., Lu, N. and Matzuk, M. M. (1996). Growth differentiation factor-9 is required during early ovarian folliculogenesis. *Nature* **383**, 531-535.

Dube, J. L., Wang, P., Elvin, J., Lyons, K. M., Celeste, A. J. and Matzuk, M. M. (1998). The bone morphogenetic protein 15 gene is X-linked and expressed in oocytes. *Mol. Endocrinol.* **12**, 1809-1817.

Durlinger, A. L., Kramer, P., Karels, B., de Jong, F. H., Uilenbroek, J. T., Grootegoed, J. A. and Themmen, A. P. (1999). Control of primordial follicle recruitment by anti-Mullerian hormone in the mouse ovary. *Endocrinology* **140**, 5789-5796.

Edelmann, W., Cohen, P. E., Kneitz, B., Winand, N., Lia, M., Heyer, J., Kolodner, R., Pollard, J. W. and Kucherlapati, R. (1999). Mammalian MutS homologue 5 is required for chromosome pairing in meiosis. *Nat. Genet.* **21**, 123- 127.

Elvin, J. and Matzuk, M. M. (1998). Mouse models of ovarian failure. *Rev. Reprod.* **3**, 183-195.

Enders, G. C. and May, J. J. 2. (1994). Developmentally regulated expression of a mouse germ cell nuclear antigen examined from embryonic day 11 to adult in male and female mice. *Dev. Biol.* **163**, 331-340.

Epifano, O., Liang, L.-F., Familari, M., Moos, M. C., Jr and Dean, J. (1995). Coordinate expression of the three zona pellucida genes during mouse oogenesis. *Development* **121**, 1947-1956.

Eppig, J. J. (1991). Intercommunication between mammalian oocytes and companion somatic cells. *BioEssays* **13**, 569-574.

Eppig, J. J., Chesnel, F., Hirao, Y., O'Brien, M. J., Pendola, F. L., Watanabe, S. and Wigglesworth, K. (1997). Oocyte control of granulosa cell development: How and why. *Hum. Reprod.* **12**, 127-132.

Gu, W., Tekur, S., Reinbold, R., Eppig, J. J., Choi, Y. C., Zheng, J. Z., Murray, M. T. and Hecht, N. B. (1998). Mammalian male and female germ cells express a germ cell-specific Y-Box protein, MSY2. *Biol. Reprod.* **59**, 1266-1274.

Halpin, D. M., Jones, A., Fink, G. and Charlton, H. M. (1986). Postnatal ovarian follicle development in hypogonadal (hpg) and normal mice and associated changes in the hypothalamic-pituitary ovarian axis. *J. Reprod. Fertil.* **77**, 287-296.

Hirshfield, A. N. (1994). Relationship between the supply of primordial follicles and the onset of follicular growth in rats. *Biol. Reprod.* **50**, 421-428.

Juneja, S. C., Barr, K. J., Enders, G. C. and Kidder, G. M. (1999). Defects in the germ line and gonads of mice lacking connexin43. *Biol. Reprod.* **60**, 1263-1270.

Kol, S. and Adashi, E. Y. (1995). Intraovarian factors regulating ovarian function. *Curr. Opin. Obstet. Gynecol.* **7**, 209-213.

Liang, L.-F., Soyal, S. M. and Dean, J. (1997). FIGa, a germ cell specific transcription factor involved in the coordinate expression of the zona pellucida genes. *Development* **124**, 4939-4949.

Littlewood, T. D. (1998). *Helix-loop-helix Transcription Factors.* New York: Oxford University Press.

Mackay, S., Nicholson, C. L., Lewis, S. P. and Brittan, M. (1999). E-cadherin in the developing mouse gonad. *Anat. Embryol.* **200**, 91-102.

Manova, K., Nocka, K., Besmer, P. and Bachvarova, R. F. (1990). Gonadal expression of c-kit encoded at the W locus of the mouse. *Development* **110**, 1057-1069.

McGrath, S. A., Esquela, A. F. and Lee, S. J. (1995). Oocyte-specific expression of growth/differentiation factor-9. *Mol. Endocrinol.* **9**, 131-136.

Millar, S. E., Lader, E., Liang, L.-F. and Dean, J. (1991). Oocyte-specific factors bind a conserved upstream sequence required for mouse zona pellucida promoter activity. *Mol. Cell. Biol.* **12**, 6197-6204.

Nagamine, C. M., Chan, K., Hake, L. E. and Lau, Y. F. (1990). The two candidate testis-determining Y genes (Zfy-1 and Zfy-2) are differentially expressed in fetal and adult mouse tissues. *Genes Dev.* **4**, 63-74.

Nagy, A., Rossant, J., Nagy, R., Abramow-Newerly, W. and Roder, J. C. (1993). Derivation of completely cell culture-derived mice from early-passage embryonic stem cells. *Proc. Natl. Acad. Sci. USA* **90**, 8424-8428.

Olson, E. N. and Klein, W. H. (1998). Muscle minus myoD. *Dev. Biol.* **202**, 153-156.

Peters, H. (1969). The development of the mouse ovary from birth to maturity. *Acta Endocrinol.* **62**, 98-116.

Pincus, G. and Enzmann, E. V. (1935). The comparative behavior of mammalian eggs *in vivo* and *in vitro*. I. The activation of ovarian eggs. *J. Exp. Med.* **62**, 655-675.

Pittman, D. L., Cobb, J., Schimenti, K. J., Wilson, L. A., Cooper, D. M., Brignull, E., Handel, M. A. and Schimenti, J. C. (1998). Meiotic prophase arrest with failure of chromosome synapsis in mice deficient for Dmc1, a germline-specific RecA homolog. *Mol. Cell* **1**, 697-705.

Porcher, C., Liao, E. C., Fujiwara, Y., Zon, L. I. and Orkin, S. H. (1999). Specification of hematopoietic and vascular development by the bHLH transcription factor SCL without direct DNA binding. *Development* **126**, 4603-4615.

Rankin, T. and Dean, J. (2000). The zona pellucida: Understanding the structure and function of the mammalian egg envelope. *Rev. Reprod.* **5**, 114-121.

Rankin, T., Familari, M., Lee, E., Ginsberg, A. M., Dwyer, N., Blanchette-Mackie, J., Drago, J., Westphal, H. and Dean, J. (1996). Mice homozygous for an insertional mutation in the *Zp3* gene lack a zona pellucida and are infertile. *Development* **122**, 2903-2910.

Rankin, T., Talbot, P., Lee, E. and Dean, J. (1999). Abnormal zonae pellucidae in mice lacking ZP1 result in early embryonic loss. *Development* **126**, 3847-3855.

Rugh, R. (1991). *The Mouse: Its Reproduction and Development.* Oxford: Oxford University Press.

Sambrook, J., Fritsch, E. F. and Maniatis, T. (1989). *Molecular Cloning: A Laboratory Manual.* Cold Spring Harbor, New York: Cold Spring Harbor Laboratory Press.

Seto, D. (1990). An improved method for sequencing double stranded plasmid DNA from minipreps using DMSO and modified template preparation. *Nucleic Acids Res.* **18**, 5905-5906.

Sun, X., Meyers, E. N., Lewandoski, M. and Martin, G. R. (1999). Targeted disruption of Fgf8 causes failure of cell migration in the gastrulating mouse embryo. *Genes Dev.* **13**, 1834-1846.

Tafuri, S. R. and Wolffe, A. P. (1990). Xenopus Y-box transcription factors: molecular cloning, functional analysis and developmental regulation. *Proc. Natl. Acad. Sci. USA.* **87**, 9028-9032.

Thomas, K. R. and Capecchi, M. R. (1987). Site-directed mutagenesis by gene targeting in mouse embryo-derived stem cells. *Cell* **51**, 503-512.

Tybulewicz, V. L. J., Crawford, C. E., Jackson, P. K., Bronson, R. T. and Mulligan, R. C. (1991). Neonatal lethality and lymphopenia in mice with a homozygous disruption of the *c-abl* proto-oncogene. *Cell* **65**, 1153-1163.

Valve, E., Penttila, T. L., Paranko, J. and Harkonen, P. (1997). FGF-8 is expressed during specific phases of rodent oocyte and spermatogonium development. *Biochem. Biophys. Res. Commun.* **232**, 173-177.

Yoshida, K., Kondoh, G., Matsuda, Y., Habu, T., Nishimune, Y. and Morita, T. (1998). The mouse RecA-like gene Dmc1 is required for homologous chromosome synapsis during meiosis. *Mol. Cell* **1**, 707-718.

Zamboni, L. and Upadhyay, S. (1983). Germ cell differentiation in mouse adrenal glands. *J. Exp. Zool.* **228**, 173-193.